JOURNAL OF CATALYSIS 80, 76–89 (1983)

Catalytic Hydrodeoxygenation

III. Interactions between Catalytic Hydrodeoxygenation of *m*-Cresol and Hydrodenitrogenation of Indole

EZEKIEL O. ODEBUNMI[1] AND DAVID F. OLLIS

Department of Chemical Engineering, University of California, Davis, California 95616

Received July 1, 1982; revised October 29, 1982

Simultaneous hydrodenitrogenation (HDN) and hydrodeoxygenation (HDO) is studied with indole/*m*-cresol conversions over a sulfided CoMo HDS catalyst. The mutual inhibition of indole (and indoline) on HDO and of *m*-cresol on HDN is established. As with HDS/HDO reported in paper II, the HDN/HDO reactions appear to proceed on the same site. The relative reactivity of the indole and cresol, as well as an HDN intermediate, *o*-ethyl aniline, is *m*-cresol $\gg$ *o*-ethyl aniline > indole (indoline). Under the conditions of our study (P_{H_2} = 69 atm, T = 250–350°C), the indole–indoline hydrogenation equilibrium is essentially achieved. The pure component conversion kinetics are adequately described by a two-site Longmuir–Hinshelwood form, the rate and binding constant values indicating correctly the relative reactivity and mutual inhibition magnitudes, thus confirming that simultaneous HDO and HDN proceed on the same surface sites. At the lower HDN temperatures, the intermediate *o*-ethyl aniline is converted to ethylbenzene, then ethylcyclohexane, while at or above 300°C some ring hydrogenation to *o*-amino ethylcyclohexane precedes HDN. Hydrogenation, HDO, and HDN activities are completely recovered by 400°C regeneration, in contrast to activity loss noted in paper II for simultaneous HDS/HDO.

INTRODUCTION

Nitrogen-containing compounds are a very significant component of shale oil, heavy gas oil, and coal-derived liquids (*1–3*). These compounds are present as pyridines, quinolines, and indoles, and are well known for their inhibiting influence on the hydrotreatment of synthetic liquid fuels and the upgrading of coal-derived liquids (*1*). Moreover, nitrogen-containing compounds are a major cause of deactivation of commercial hydrotreating catalysts, and are responsible for the instability of finished liquid products (*3*). Thus they are a focus of extensive studies and recent reviews (*1, 2*).

The few literature reports on HDO and HDN reactions do not specifically address the subject of the influence of oxygen-containing species on the HDN reaction (*2, 4–6*). In general, inhibition of all other reactions by nitrogen-containing compounds is reported. Some of the studies investigated simultaneous S, N, and O removal from model feed mixtures (*4, 5*) and others addressed real feedstocks (*6, 7*). Most of the literature reports on HDN are on pyridine (*8–10*) and quinoline HDN (*11–13*), and a few deal with indole HDN (*4, 5, 13*). The reaction network for indole HDN is not as unambiguously defined as HDN of others, although it may be less complicated.

By comparison with HDS, catalytic HDN is a complicated process involving hydrogenation, hydrocracking, hydrogenolysis, and alkyl transfer reactions. McIlvried (*8*) investigated the kinetics of pyridine HDN by Ni–Co–Mo/alumina catalysts in a bench-scale, fixed-bed flow reactor at 315°C and pressures of 51 to 102 atm. His data were fitted to a Langmuir–Hinselwood kinetic model, in which competitive

[1] On leave from Princeton University. Present address: Department of Chemical Engineering, University of Delaware, Newark, Delaware 19711.

0021-9517/83/030076-14$03.00/0

inhibition of the HDN reaction by the products was assumed. In a series of experimental studies, Sonnemans and co-workers (*9*) investigated the hydrogenation and hydrogenolysis of pyridine on reduced but unsulfided Co–Mo/alumina catalysts. They observed alkyl transfer reactions resulting in formation of *N*-pentylpiperidine. Analogous disproportionation reactions have not been observed during quinoline HDN reaction.

In another report Satterfield *et al.* (*11*) studied the intermediate reactions in the vapor-phase HDN of quinoline on a sulfided $NiMo/Al_2O_3$ catalyst in a continuous-flow microreactor. The experiments proceeded at 230 to 420°C and at pressures of 34 to 68 atm. Gates *et al.* (*12*) also studied the HDN of quinoline and coal-derived liquids. These studies show that the hydrogenolysis of *o*-propylaniline, an intermediate in quinoline HDN, is one of the principal rate-limiting steps, whereas in pyridine HDN, *n*-pentylamine is rapidly denitrogenated (*8, 11*).

Indole HDN appears to proceed via a series of consecutive reaction steps, although two different reaction paths are reported for the denitrogenation of *o*-ethylaniline (an intermediate in indole HDN) to form ammonia and hydrocarbon (*4, 5, 13*). Rollmann (*4*) observed saturation of the aromatic nucleus of the amine prior to nitrogen removal for reaction at 350 to 400°C. Aboul-Gheit and Abdou (*13*) and Whitehurst *et al.* (*5*) (for reactions at 350–400°C), on the other hand, reported hydrocracking of the aromatic carbon–nitrogen bond leading to formation of ammonia before saturation of the aromatic nucleus. Thus the products and reaction network for HDN depend on the nitrogen-containing compounds and the reaction condition. In general the HDN reaction is reported to be first order in the organic compound (*1, 2*).

The experiments reported in the present paper investigated the HDO and HDN of *m*-cresol-only and indole-only reactant feeds, the influence of *m*-cresol on the HDN of indole, and the influence of indole on the HDO of *m*-cresol in mixed *m*-cresol–indole feeds. Indole was chosen as the nitrogen-containing compound for these experimental studies.

EXPERIMENTAL METHODS

The experimental procedures for the HDO and HDN runs and sample analysis follow those described in the previous papers (*20, 21*). Chemical reagents were used as received from Aldrich Chemicals Company without further purification. The catalysts used in these experiments are those described as freshly sulfided Co–Mo catalysts II in paper I (*20*).

The catalyst was activated prior to use in these runs by reduction in hydrogen followed by sulfiding in H_2/H_2S gas mixture (10 vol% H_2S) for 4 hr. Catalyst regeneration was repeated after several weeks of continuous use; this treatment of high-temperature reduction in hydrogen followed by resulfiding in H_2/H_2S mixture completely restored catalyst activity.

Each reactant feed contained 0.15 *M m*-cresol, 0.0075 *M n*-heptyl mercaptan, and varying amounts of indole. Several runs investigated the influence of initial feed concentration of the HDO of *m*-cresol and HDN of indole. Conversion and relative rate data were also obtained for pure feedstocks of *m*-cresol, indole, and *o*-ethylaniline to allow comparison of the HDO and HDN results in the single- and mixed-feed cases. The HDN conversion was defined as Σ(all N-free ethyl (benzene + cyclohexane)) divided by the feed indole level.

The HDO and HDN experiments were done at 250–350°C, 69 atm H_2 pressure, 120 cm^3 (STP)/min H_2 flow and reactant liquid flow rates of 4.5 to 12.5 cm^3/hr. The trickle-bed reactor which has been fully described in paper I (*20*) was used for all the experimental runs. Reactant feed and product samples were analyzed by gas chromatography, and gas chromatography–mass spectrometry (GC–MS) was used to establish products unambiguously.

RESULTS

HDO of m-Cresol

In the presence of indole, the HDO of *m*-cresol gives toluene and methylcyclohexanes as major products. The relative distribution of the *m*-cresol HDO products does not appear to depend on the level of indole in the reactant feed. The indole-free runs D4 and D12 provide linear $\ln(1 - X)$ plots vs reciprocal space velocity, *W/F* (Fig. 1 and Table 1). The indole–cresol runs D_5, D_8, D_9, and D_{10} exhibit a definite curvature, as well as N inhibition. As the indoline/indole ratio also changes with flow rate (Table 2a), these results indicate a somewhat stronger inhibition by indoline than by indole. Removal of indole (run D_{11}) restored only half of the original activity (D_4); regeneration fully restored the original HDO activity as seen in (D_{12}).

At the higher temperatures (275–300°C) the *m*-cresol deoxygenation again decreased as the feed concentration of indole

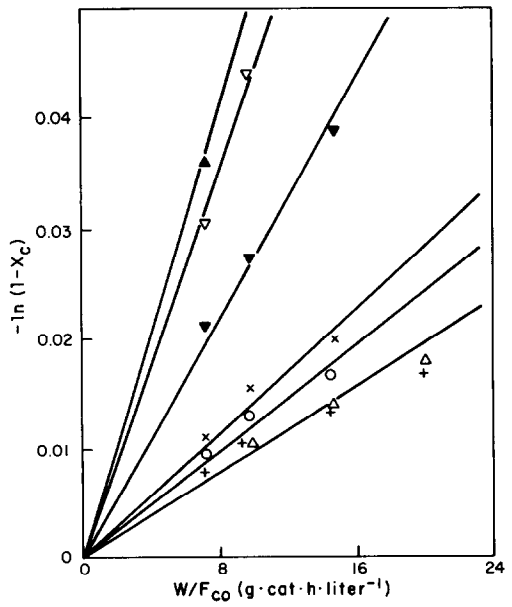

FIG. 1. Indole inhibition of *m*-cresol HDO. T = 250°C, *m*-cresol = 0.15 *M*, P_{H_2} = 69 atm. Indole concn: 0.0 *M* (D_4, ▽), 0.0075 *M* D_5, △), 0.005 *M* (D_8, +), 0.0025 *M* (D_9, ○), 0.001 *M* (D_{10}, ×), 0.0 *M* (D_{11}, no prior regeneration, ▼), 0.0 *M* (D_{12}, after regeneration, ▲). See Table 1.

TABLE 1

Effect of Indole on the HDO of 0.15 *M* *m*-Cresol at 250°C

Reactant liquid flow rate V_{0_5} (cm³/hr)	Percentage *m*-cresol conversion $X_c = \left(\frac{[MCH] + [TOL]}{[cresol]}\right) \times 100$						
	D_4 —	D_{10} 0.001 *M* IND	D_9 0.0025 *M* IND	D_8 0.005 *M* IND	D_5 0.0075 *M* IND	D_{11} —	D_{12} —
4.5	9.6	2.5	2.0	1.6	1.8	4.6	10.7
6.1	6.9	2.0	1.7	1.4	1.4	3.8	8.4
9.2	4.3	1.5	1.3	1.0	1.0	2.7	5.5
12.5	3.0	1.	0.9	0.8	0.8	2.1	3.6
$10^4 k_{HDO}$ liter · (hr · g · cat)$^{-1}$	49.1 ± 0.3	14.1 ± 1.5	12.1 ± 0.9	9.8 ± 0.7	10.0 ± 0.9	27.1 ± 0.3	56.0 ± 0.2

TABLE 2a

Indole–Indoline Hydrogenation Equilibrium at 250°C

Reactant liquid flow rate V_0 (cm³/hr)	$\frac{[\text{indoline}]}{[\text{indole}]} = K_e (P_{H_2})$				
	D_5 0.001 *M* IND	D_8 0.0025 *M* IND	D_9 0.005 *M* IND	D_{10} 0.0075 *M* IND	D_6[a] 0.0075 *M* IND
4.5	1.22	1.43		0.81	1.28
6.1	1.45	1.21	1.99	0.91	1.08
9.2	1.31	1.11	1.58	0.43	0.96
Mean $\frac{[\text{indoline}]}{[\text{indole}]}$	1.22	1.19	1.64	0.82	1.04

[a] Experiment D_6 reactant feed contained only indole + mercaptan in *n*-hexadecane; all the other experiments contained 0.15 *M* *m*-cresol as well as indole and mercaptan.

TABLE 2b

Indole–Indoline Ratio at 275°C

Reactant liquid flow rate V_0 (cm³/hr)	$\frac{[\text{indoline}]}{[\text{indole}]}$				
	E_2 0.025 *M* IND	E_3 0.005 *M* IND	E_4 0.0075 *M* IND	E_5 0.015 *M* IND	E_6 0.15 *M* IND
4.5	1.08	1.36	1.29	1.12	0.85
6.2	1.11	1.40	1.25	1.04	0.81
9.4	1.01	1.26	1.15	0.98	0.75
12.6	1.12	1.30	1.14	0.93	0.73
Mean $\frac{[\text{indoline}]}{[\text{indole}]}$	1.08	1.33	1.21	1.02	0.79

Note. Excepting those in brackets, all data refer to mixed-reactant feeds containing 0.15 *M* *m*-cresol.

TABLE 2c

Indole–Indoline Ratio at 300°C

Reactant liquid flow rate V_0 (cm³/hr)	$\frac{[\text{indoline}]}{[\text{indole}]}$			
	F_2 0.005 *M* IND	F_3 0.0075 *M* IND	F_4 0.015 *M* IND	F_5 0.15 *M* IND
4.4	0.95	0.80	0.76	0.53
6.2	1.17	0.87	0.77	0.53
9.3	0.98	0.77	0.70	0.51
12.5	0.96	0.75	—	0.50
Mean $\frac{[\text{indoline}]}{[\text{indole}]}$	0.96	0.80	0.74	0.52

Note. Excepting those in brackets, all data refer to mixed-reactant feeds containing 0.15 *M* *m*-cresol.

in the mixed reactant feed increased (Figs. 2 and 3).

The presence of linear $\ln(1 - X_{HDO})$ plots vs W/F_{co} (Figs. 2 and 3) corresponds nicely to essentially constant indoline/indole ratios independent of space velocity (Tables 2b and c).

Comparison of our HDO–HDN data with the HDO–HDS data of paper II (*21*) shows that indole has a significantly stronger inhibition per mole on the HDO reaction than do corresponding levels of benzothiophene or dibenzothiophene.

Indole–indoline hydrogenation equilibrium. The CoMo-catalyzed hydrogenation of indole gave predominantly indoline as the product. Our data at 275–300°C (Tables 2b to d) show that the ratio of indole to indoline appears to be approximately constant, strongly suggesting an equilibration.

The indole–indoline ratio shows a strong dependence on temperature, shifting in favor of indole as the temperature is raised (Table 2d), in agreement with the expected behavior of an equilibrated reaction:

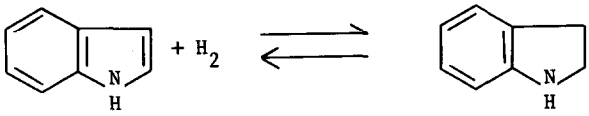

Satterfield *et al.* (*11*) have reported that in the HDN of quinoline, the tetrahydroquinoline–quinoline equilibrium ratio shifts in favor of quinoline as the temperature is raised. Sonnemans *et al.* (*9*) made a similar observation for tetrahydropyridine–pyridine ratio during pyridine HDN.

HDN of indole/indoline. As noted earlier the hydrogenation of indole is faster than the HDN reaction at the temperatures (250–350°C) of our study, and especially at the lowest temperature. The rate of indole HDN is very small at 250°C, but it increases to significant levels as the temperature is raised to 275 and 300°C. The major products of the indole conversions include *o*-ethylaniline and ethylbenzene. Ethylcyclohexenes and ethylcyclohexane were formed in relatively small quantities at the lower temperatures (250–275°C), but the rate of their production increased at the higher temperatures (300–350°C). Also

TABLE 2d

Indole–Indoline Hydrogenation Equilibrium

Reactant liquid flow rate V_0 (cm³/hr)	$\frac{[\text{indoline}]}{[\text{indole}]} = \alpha \cong K_e (P_{H_2})$				
	275°C		300°C		350°C
	IND[a] 0.15 *M*	CRE/IND[b] 0.15 *M*	IND 0.15 *M*	CRE/IND 0.15 *M*	IND 0.15 *M*
4.5	0.79	0.85	0.55	0.53	0.26
6.1	0.70	0.81	0.54	0.53	0.26
9.2	0.73	0.75	0.52	0.51	0.26
12.4	0.75	0.73	0.47	0.50	0.23
Mean $\bar{\alpha}$	0.74	0.79	0.52	0.52	0.25

[a] IND means indole-only feed.

[b] CRE/IND means mixed (equimolar) cresol–indole feed.

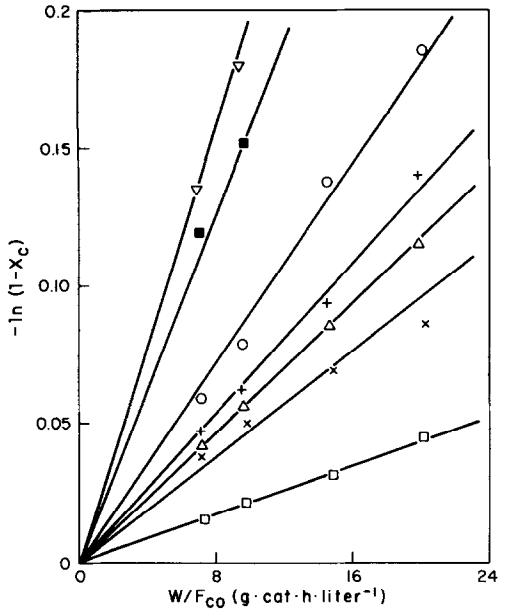

FIG. 2. Indole inhibition of *m*-cresol HDO. T = 275°C, *m*-cresol = 0.15 M, P_{H_2} = 69 atm. Indole concn: 0.0 M)E_1, ▽), 0.0036 M (E_2, ○), 0.005 M (E_3, +), 0.0075 M (E_4, △), 0.015 M (E_5, ×), 0.15 M (E_6, □), 0.0 M (E_7, no prior regeneration, ■).

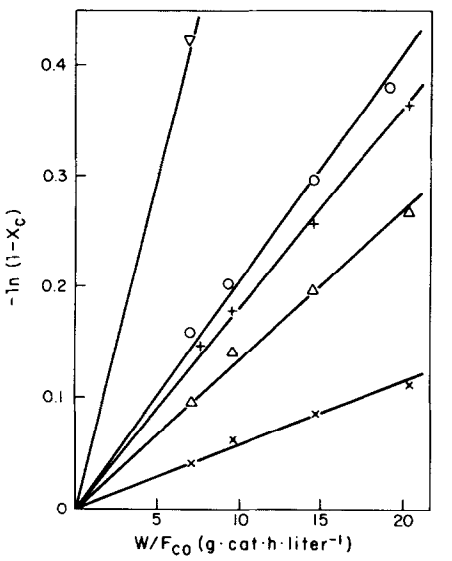

FIG. 3. Indole inhibition of *m*-cresol HDO. T = 300°C, *m*-cresol = 0.15 M, P_{H_2} = 69 atm. Indole concn: 0.0 M (F_1, ▽), 0.005 M (F_2, ○), 0.0075 M (F_3, +), 0.015 M (F_4, △), 0.15 M (F_5, ×).

some quantities of *o*-aminoethylcyclohexane were formed at the higher temperatures (300–350°C).

The results in Tables 3a and b clearly show the *m*-cresol inhibition of indole HDN. The inhibiting influence of *m*-cresol results in 20 and 60% reduction of the HDN rates at 275 and 300°C, respectively, for mixed feeds containing 0.015 M indole and 0.15 M *m*-cresol. This inhibiting influence of *m*-cresol appears to be much weaker for reactant feeds containing equimolar (0.15 M each) cresol–indole at 300°C (Table 3b) and is nonexistent at 275°C (Table 3a, last two columns). Thus, although *m*-cresol inhibits the HDN reaction, the inhibition effect is not important at higher indole concentrations, whereas the indole/indoline inhibition of cresol HDO is dominant under

TABLE 3a

Effect of *m*-Cresol on the HDN of Indole at 275°C

Reactant liquid flow rate V_0 (cm³ hr)	Percentage conversion $X_N = \left(\frac{[\Sigma \text{ C products}]}{[C_{\text{indole}(0)}]}\right)$			
	G_6 Indole 0.015 M	F_6 CRE/IND 0.15 M/0.015 M	G_4 Indole 0.15 M	E_6 CRE/IND 0.15 M/0.15 M
4.5	13.6	10.1	2.3	2.3
6.1	9.8	7.7	1.3	2.0
9.3	6.4	5.7	0.8	1.5
12.4	3.80	3.4	0.6	1.2
$10^4\ k'_{HDN}$ liter · (hr · g · cat)$^{-1}$	6.63 ± 0.76	5.31 ± 0.44	1.03 ± 0.14	1.34 ± 0.36

TABLE 3b

Effect of *m*-Cresol on the HDN of Indole at 300°C

Reactant liquid flow rate V_0 (cm³ hr)	Percentage conversion $X_N = \left(\frac{[\Sigma \text{ C products}]}{[C_{\text{indoline}(0)}]}\right)$			
	G_1 Indole 0.015 *M*	F_4 CRE/IND 0.15 *M*/0.015 *M*	G_3 Indole 0.15 *M*	F_5 CRE/IND 0.15 *M*/0.15 *M*
4.5	57.3	24.9	5.3	5.3
6.1	40.8	22.80	4.9	4.2
9.3	29.0	17.7	4.1	3.0
12.4	21.2	—	3.2	2.5
$10^3 k'_{HDN}$ liter · (hr · g · cat)$^{-1}$	39.34 ± 3.54	15.68 ± 2.45	3.78 ± 0.45	3.11 ± 0.70

these conditions (e.g., compare E_1 vs E_6, Fig. 2 and F_1 vs F_5, Fig. 3).

Table 4 compares the conversion and distribution of products during the HDN of (a) indole-only feed (G_3), (b) mixed cresol–indole feed (F_5), (c) *o*-ethylaniline (G_5), all at 300°C, and the HDN of indole at 350°C (G_8). The presence of *m*-cresol in the mixed feed has no effect on the distribution of indoline and indole but it reduces the ratio of the hydrogenation products (ethylcyclohexanes/ethylbenzene). Also, both this ratio as well as the HDN rate are higher for *o*-ethylaniline versus indole. As the temperature increases to 350°C, the indole HDN rate and the ratio of the hydrogenated/aromatic products both increase, but the ratio of indoline to indole decreases drastically. These behaviors are consistent with kinetic and thermodynamic limitations, respectively.

Several experiments investigated further saturation of the HDN rate by indole and similar saturation of the HDO rate by *m*-cresol (Figs. 4 and 5). The results, summarized in Fig. 6, show that the apparent first-order rate constants k'_{HDO}, k'_{HDN} decrease as the concentration of *m*-cresol and indole, respectively, in the reactant feed increase. Thus the HDO and HDN active sites are approaching saturation in *m*-cresol and indole, respectively. In a recent paper, Gates and Broderick (*19*) report a tendency toward saturation of the HDS active sites by dibenzothiophene during the HDS of BT. Interestingly, McIlvried (*8*) and Sonnemans *et al.* (*9*) reported self-inhibition of the HDN of pyridine.

Relative Rates of HDO and HDN Reactions

The data in Table 5 compare the rate of HDO of *m*-cresol with the rates of indole and *o*-ethylaniline HDN at 275 and 300°C. First-order plots from these data (ln (1 − *X*)

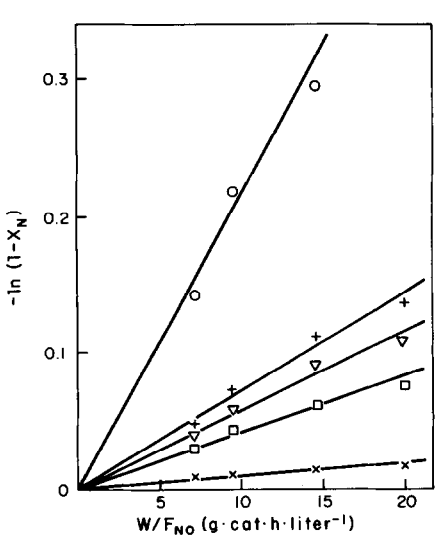

FIG. 4. Indole HDN with simultaneous *m*-cresol HDO. T = 275°C, *m*-cresol = 0.15 *M*, P_{H_2} = 69 atm. Indole concn: = 0.0025 *M* (E_2, ○), 0.005 *M* (E_3, +), 0.0075 *M* (E_4, ▽), 0.015 *M* (E_5, □), 0.15 *M* (E_6, ×).

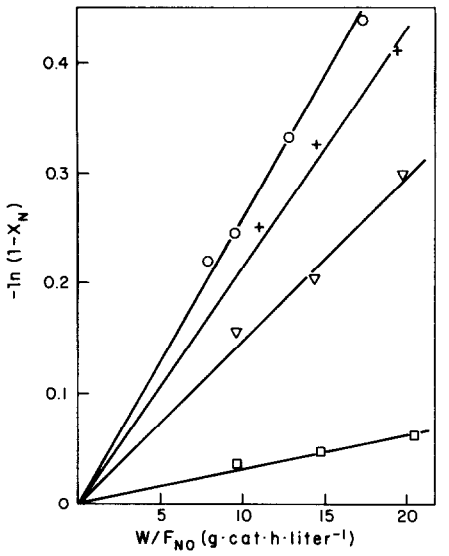

FIG. 5. Indole HDN with simultaneous *m*-cresol HDO. T = 300°C, *m*-cresol = 0.15 M, P_{H_2} = 69 atm. Indole concn: 0.005 M (F_2, ○), 0.0075 M (F_3, +), 0.015 M (F_4, ▽), 0.15 M (F_5, □).

vs W/F) give the apparent first-order rate constants of the bottom row, Table 5. The *m*-cresol is by far the most reactive of the three; the following decreasing order of reactivity is indicated:

m-cresol ≫ *o*-ethylaniline > indole (indoline*).

(*Indole and indoline form an equilibrium mixture for these runs.)

Catalyst Deactivation

A gradual loss of HDO activity of the CoMo catalyst was observed following each series of HDO–HDN runs, as is seen by comparing runs at identical conditions, e.g., runs D_4 and D_{11} in Fig. 1 and runs E_1 and E_7 in Fig. 2. These two sets of experiments show that about 45 and 20% loss of catalyst activity, respectively, was observed following HDO–HDN runs at 250 and 275°C, respectively. In both cases the activity loss was completely regenerated by high-temperature (400°C) rereduction in hydrogen and resulfiding in H_2/H_2S mixture. (Compare the regenerated catalyst activi-

TABLE 4

Conversion and Product Distribution in HDN Reactions

Reactant liquid flow rate V_0 (cm³/hr)	(G_3) Indole only 300°C			(F_5) Cresol–indole 300°C			(G_5) *o*-Ethyl aniline 300°C			(G_8) Indole 350°C		
	%X_N	$\frac{[INDE]^a}{[IND]}$	$\left(\frac{ET_1 + ET_2}{ETBZ}\right)^b$	%X_N	$\frac{[INDE]^a}{[IND]}$	$\left(\frac{ET_1 + ET_2}{ETBZ}\right)^b$	%X_N	$\frac{[INDE]^a}{[IND]}$	$\left(\frac{ET_1 + ET_2}{ETBZ}\right)^b$	%X_N	$\frac{[INDE]^a}{[IND]}$	$\left(\frac{ET_1 + ET_2}{ETBZ}\right)^b$
4.5	5.3	0.55	0.66	5.3	0.53	0.50	9.9		1.24	47.4	0.26	1.11
6.1	4.9	0.54	0.70	4.2	0.53	0.49	5.9		1.00	41.0	0.26	0.99
9.2	4.1	0.52	0.62	3.0	0.51	0.47	4.2		0.79	31.3	0.26	1.01
12.4	3.2	0.47	0.61	2.5	0.50	0.46	3.0		0.70	20.2	0.23	1.18
$10^3 k_{HDN}$ liter · (hr · g · cat)⁻¹		3.78 ± 0.45			3.11 ± 0.09			4.70 ± 0.52			33.86 ± 5.25	

Note. Only Expt. F_5 contained 0.15 M *m*-cresol; all the others contained either only indole or only *o*-ethyl aniline (9.15 M). ETBZ = ethyl benzene.

[a] [INDE] = indoline, [IND] = indole.

[b] ET_1, ET_2 = ethylcyclohexene, ethylcyclohexane.

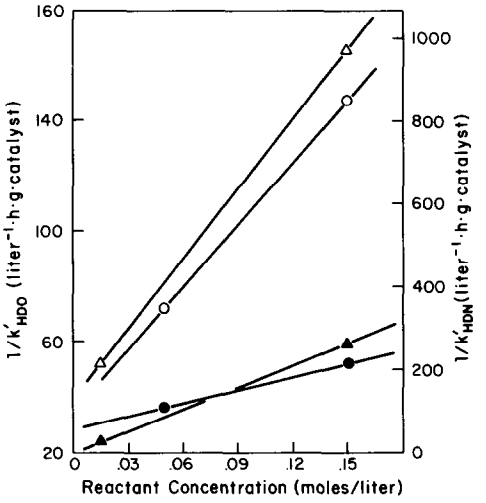

FIG. 6. Inverse of apparent first-order rate constant vs feed reactant concentration. *m*-Cresol HDO: T = 250°C (○), T = 275°C (●); indole HDN: T = 275°C (△), T = 300°C (▲).

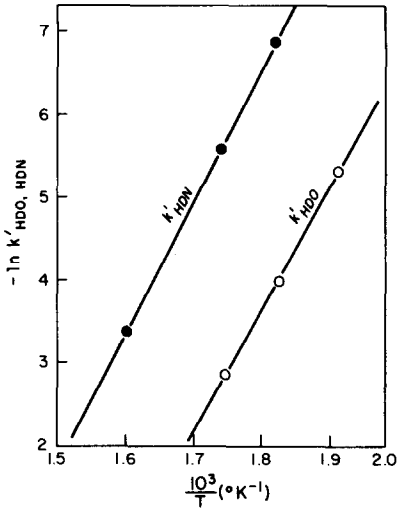

FIG. 7. Arrhenius plot for pure component apparent first-order rate constants. *m*-Cresol (○), indole (●).

ties (D_{12}, Table 1). Thus, to ensure that an average constant catalyst activity was maintained, the catalyst regeneration treatment was done after every several weeks of continuous use.

DISCUSSION

Kinetic Analysis

As noted earlier, the HDO and HDN reactions exhibit apparent first-order behavior in the organic reactant for both the single and mixed feedstocks. Logarithmic plots of the pseudo-first-order rate constants (k'_{HDO}, k'_{HDN}) against the reciprocal temperature (°K^{-1}) yielded the apparent activation energies and frequency factors. These plots are shown in Fig. 7. Linear least-squares regression analysis gives "activation energies" of 29 and 32 kcal/mole for *m*-cresol HDO and indole HDN, respec-

TABLE 5

Relative HDO and HDN Rates

Reactant liquid flow rate V_0 (cm³/hr)	275°C		300°C		
	m-Cresol X_c[a] (E_1)	Indole X_N[a] (G_4)	*m*-Cresol X_c[a] (F_1)	Indole X_n[a] (G_3)	*o*-Etha[b] X_N (G_5)
4.5	30.7	2.3	65.1	5.34	9.9
6.1	25.1	1.3	56.1	4.90	5.9
9.2	16.4	0.8	41.7	4.10	4.2
12.4	12.6	0.6	34.4	3.20	3.0
10^4 k'[c] liter · (hr · g · cat)$^{-1}$	190.0	10.3	565.6	37.8	47.0

[a] Conversion X is defined as the ratio of the products to the initial reactant concentration.
[b] *o*-Etha refers to *o*-ethylaniline.
[c] k' is pseudo-first-order rate constant in liters hr^{-1} g^{-1} of catalyst.

tively, with a correlation coefficient of 99.9%. The ln A values were 22.7 and 22.2 liters-hr^{-1}/(g-cat)$^{-1}$, respectively.

For formulation of a kinetic model for the HDO–HDN coupling interactions we combine our observations with information available in the literature. The major observations from our HDO–HDN data can be summarized as follows:

(i) Indole inhibits the HDO of *m*-cresol.

(ii) *m*-Cresol inhibits the HDN of indole.

(iii) The pseudo-first-order rate constants for HDO and HDN (k'_{HDO}, k'_{HDN}) decreased as the reactant (*m*-cresol, indole) concentration increased.

(iv) *m*-Cresol is more reactive to deoxygenation on the Co–Mo catalysts than indole is to denitrogenation.

(v) The indole–indoline hydrogenation equilibrium appears to be approximately attained at all conditions. The subsequent hydrogenolysis reactions leading to the formation of *o*-ethylaniline and ethylbenzene under our reaction conditions (250–300°C, 69 atm hydrogen pressure) limit the rate of HDN.

McIlvried (*8*) investigated the HDN of pyridine and piperidine on sulfided CO–Ni–Mo catalysts supported on alumina at 316°C temperature and pressures of 51 to 102 atm. In a series of experiments Sonnemans *et al.* (*9*) studied the hydrogenation and hydrogenolysis of pyridine on unsulfided Mo alumina and Co–Mo alumina catalysts at 250–375°C. Both authors developed rate expressions for the hydrogenation and HDN reactions that assume strong adsorption of reactants and products. McIlvried (*8*) assumed that both reactants and products are equally strongly adsorbed. The adsorption and other studies of Sonnemans and co-workers (*9*) indicate different binding sites for the organic nitrogen compounds and hydrogen. In a recent report Satterfield and co-workers (*15, 16*) concluded that there are large variations among the relative adsorptivities of the various N-containing species present during the HDN of quinoline on sulfided NiMo/Al_2O_3 catalysts. We noted earlier that indoline may bind somewhat more strongly than indole.

For simplicity, a Langmuir–Hinshelwood kinetic model is proposed for the HDO–HDN data similar to that used for analysis of the HDO–HDS data of paper II. This model assumes two nonidentical sites for the HDN reaction, with competitive adsorption of the reactants (*m*-cresol and indole) and their conversion products on one of these sites. Hydrogen is noncompetitively adsorbed on the other sites. In this picture indole and its conversion products (*o*-ethylaniline, NH_3) are assumed to have the same binding constant K_N. This approach is conceptually identical to that used in paper II for simultaneous HDO/HDS.

Thus rate equations are again written for four different cases, including:

(a) HDO of *m*-cresol in cresol-only feed.

(b) HDO of *m*-cresol in mixed cresol–indole feed.

(c) HDN of indole in indole-only feed.

(d) HDN of indole in mixed cresol–indole feed.

For case (d), for example, the HDN rate is given by

$$F_{NO}\frac{dX_N}{dW} = \frac{k_{HDN}K_N C_{NO}(1 - X_N)}{1 + K_C C_C + K_S C_s + K_N C_N},$$

where $K_S C_S$ represents the inhibition term for H_2S formed from desulfurization of trace mercaptan present in all reactant feeds.

In making the final calculations, we assumed that the inhibition term for H_2S ($K_S C_S$) is negligible, at least for the HDN reaction, under the conditions of our experiments. Satterfield and Cochetto (*10*) observed enhancement of the HDN of pyridine by thiophene and H_2S. Goudriaan *et al.* (*14*) studied the effects of presulfiding Co–Mo/alumina catalyst and of the presence of hydrogen sulfide on the hydrodenitrogenation of pyridine at 80 atm pressure and temperatures of 250–400°C. They concluded that hydrogen sulfide has a twofold

beneficial effect on pyridine HDN; it enhances both hydrogenation and hydrocracking activity of the catalyst. In another report, Satterfield and Gültekin (*16*) have shown that for quinoline HDN, H_2S has a slight inhibiting effect on the intermediate hydrogenation steps but a marked accelerating effect on the overall HDN rate.

Neglecting small C_N and C_C variations, the apparent first-order rate constant k'_{HDN} derived from the slope of $-\ln(1 - X)$ vs W/F plots is given by

$$1/k'_{HDN} = \left(\frac{1 + K_C C_{CO} + K_N C_{NO} + K_S C_S}{k_{HDN} K_N}\right).$$

From appropriate plots (e.g., $1/k'_{HDN}$ vs C_{NO}) from this equation and the other three equations representing the remaining three cases (see Odebunmi (*22*)), the true rate constant for the HDN reaction (k_{HDN}) and the equilibrium adsorption coefficients (K_N, K_c) can be calculated. The plots are shown in Fig. 6 for the cresol-only and indole-only feeds and in Fig. 8 for the mixed cresol–indole feeds.

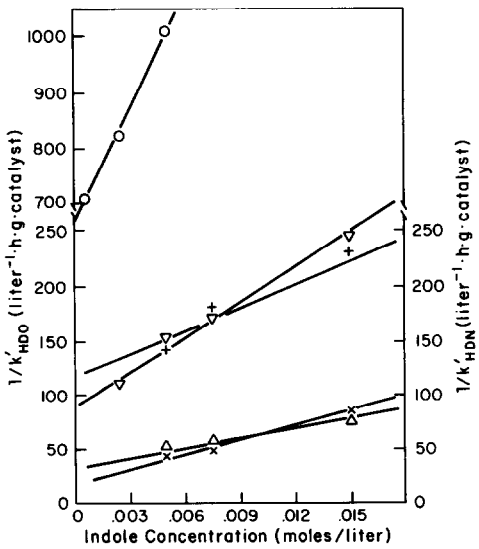

FIG. 8. Indole inhibition: influence on apparent first-order rate constants in mixed-feed experiments. *m*-Cresol = 0.15 *M*. T = 250°C, HDO (○); T = 275°C (HDO (▽), HDN (+)), T = 300°C (HDO (△), HDW (×)).

The parameter results are summarized in Table 6; they show that indole and its conversion products (indoline) are more strongly bound than *m*-cresol and its conversion products (water).

The apparent activation energies measured for *m*-cresol HDO and indole HDN are 29 and 32 kcal/mole, respectively (Table 6), versus 26 (for *p*-cresol) and 28 (for indole) kcal/mole as determined by Rollmann (*4*). Aboul-Gheit and Abdou (*13*) reported an activation energy of indole HDN as 18 kcal/mole.

In our experiments we found that the catalyst activity loss following a series of HDO–HDN runs at the low temperatures (250–275°C) was completely regenerated by high-temperature reduction and sulfiding. (Compare D_4, D_{11}, and D_{12} in Table 1, and E_1, E_7, and E_8 in Fig. 3.) No such deactivation was observed at the higher temperatures (300°C and above). By contrast the activity loss following HDO–HDS runs (paper II (*21*)) was not completely restored by reduction and resulfiding.

Interactions of HDO/HDN and HDO/HDS Reactions, and Relative Reactivities

The mutual inhibition of the HDO–HDN reactions by *m*-cresol, indole, and their conversion products is a very significant result. The relative magnitudes of the binding constants show why indole has a greater effect on the *m*-cresol HDO than *m*-cresol has on the indole HDN reactions. In paper II (*21*) we reported a similar mutual inhibition of the HDO–HDS reactions by *m*-cresol, benzothiophene (BT), dibenzothiophene (DBT), and their conversion products. Furthermore, we found that BT and DBT have greater inhibiting influence on *m*-cresol HDO than *m*-cresol has on their HDS. However, in mixed-reactant feeds containing disproportionately higher oxygen-containing compounds, the inhibition of the other reactions by O compounds may become important. Thus in the cata-

lytic upgrading of coal-derived liquids, closer attention should be paid to the influence of oxygen-containing species on catalyst performance and on the overall process.

The results of our experiments show that for the N, O, S compounds involved in our studies, the hydrodesulfurization (HDS) reaction is faster than the hydrodeoxygenation (HDO) reaction, and this in turn is faster than the hydrodenitrogenation (HDN) reaction. The relative carbon–carbon, carbon–nitrogen, carbon–sulfur, and carbon–oxygen bond strengths (Table 7) partially explain the differences in difficulty of HDS, HDN, and HDO reactions (*6*). The bond strength of the carbon–heteroatom (C–X, X = N, S, O) bond increases in the order sulfur, nitrogen, and oxygen. In agreement with expectation from C–X bond strength order, Satterfield and Cochetto (*10*) found the catalytic pyridine HDN to be more difficult than thiophene HDS. In a more recent report Furimsky (*6*) noted that the relative rates of simultaneous S, N, and O removal from a heavy gas oil are in the decreasing order C–S > C–N > C–O, based on heterocyclic compounds. However, from studies with model feed mixtures (of N, S, and O compounds), Rollmann (*4*) proposed a different order of reactivity that does not follow the order of the C–X bond strength: *p*-alkyphenols are argued to be more reactive to HDO than benzothiophenes are to HDS, and these in turn are more reactive than indoles to HDN.

Reaction network for indole HDN. The distribution of indole HDN products suggests a sequence involving hydrogenation of the nitrogen-containing ring as the first step. This is followed by hydrocracking of the C–N bond to form *o*-ethylaniline. The eventual hydrocracking of the second C–N bond produces ammonia (NH_3) and ethylbenzene, with the latter undergoing partial hydrogenation to ethylcyclohexene and ethylcyclohexane. At the higher temperatures of our study (300–350°C) another reaction involving hydrogenation of the aromatic ring of the *o*-ethylaniline competes with the second C–N hydrogenolysis rate. The aromatic ring hydrogenation gives *o*-amino ethylcyclohexane which then loses ammonia to form ethylcyclohexane. Therefore we will use the following reaction network, which has support, for the hydrodenitrogenation of indole:

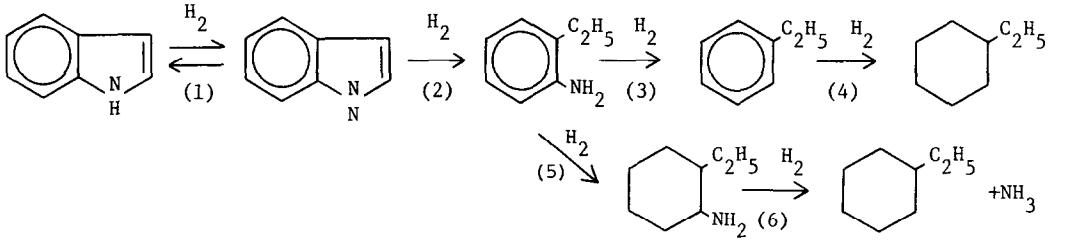

Under our reaction conditions (250–350°C, 69 atm H_2 pressure) the second step of this network is the rate-determining step for overall hydrodenitrogenation, in agreement with literature reports (*4, 13*). Moreover, indole and indoline appear to be in thermodynamic equilibrium, with the equilibrium shifting in favor of indole as the temperature increases. Following the heterocyclic ring opening, the consecutive steps (3) and (4) were observed by Whitehurst *et al.* (*5*) and Aboul-Gheit and Abdou (*13*). They did not observe steps (5) and (6). Rollmann (*14*), on the other hand, reported over 90% selectivity to alkylcyclohexane (via steps (5) and (6)) at 344°C on CoMo catalysts. This selectivity decreased to 74% at 399°C. As mentioned earlier, steps (5)

TABLE 6

True Rate Constants and Equilibrium Adsorption Coefficients for *m*-Cresol and Indole

Temperature (°C)	*m*-Cresol		Indole	
	$10^4\ k_{HDO}$ (moles(hr · g · cat)$^{-1}$)	K_c (liters/mole)	$10^4\ k_{HDN}$ (moles(hr · g · cat)$^{-1}$)	K_N (liters/mole)
250	13.4	21.1	1.1	2172.5
275	62.6	5.6	2.5	79.6
300	254.9	1.7	5.3	3.7
350	3006.4	—	20.2	—
E_a[a] or ΔH	35.0	30.2	20.0	76.0
ln A[b] or $\Delta S/R$	27.0	26.0	10.0	65.4

[a] E_a and ΔH are in kcal/mole. ΔH refers to K_c and K_N.

[b] $\Delta S/R$ refers to K_c and K_N. For K_c and K_N we used:

$$\Delta G = \Delta H - TS = -RT \ln K;\ \ln K = \frac{-\Delta G}{RT} = \left(\frac{\Delta S}{R} - \frac{\Delta H}{RT}\right).$$

and (6) in our studies did not become significant until higher temperatures (300°C and above).

CONCLUSIONS

Indole (indoline) inhibits the HDO of *m*-cresol. To a lesser degree, *m*-cresol similarly inhibits the HDN of indole. The HDO–HDN conversion data are fitted by a relatively simple Langmuir–Hinshelwood kinetic model, similar to that used to describe the HDO–HDS data (paper II). The simple kinetic expressions assume equal competition for the oxygen binding sites by indole and indoline, its hydrogenation products.

TABLE 7

Bond Energies between Carbon and Heteroatoms in Polyatomic Molecules (*17, 18*)

Bond	Energy (kcal/mole)
C—H	99
C—C	83
C=C	148
C≡C	194
N—H	93
C—N	70
C=N	147
C≡N	210
C—S	65
C=S	128
S—H	83
C—O	82
C=O	169
O—H	110

The analysis of the data yields the true rate constants k_{HDO}, k_{HDN} for hydrodeoxygenation and hydrodenitrogenation reactions, respectively, as well as the binding constants K_C, K_N for *m*-cresol and indole, respectively. The magnitude of the binding constants and the heats of adsorption for *m*-cresol and indole deduced from pure component HDO and HDS experiments explain the greater inhibiting influence of HDO by indole versus the inhibition of the HDN reaction by *m*-cresol, provided both conversions occur on the same site. The moderate inhibition of the HDN reaction by *m*-cresol may become yet more significant in a real feedstock (e.g., coal-derived liquids) which contains (i) significantly more oxygen-containing cresol species than nitrogen-containing compounds, or (ii) more stable oxygenates than cresols (e.g., benzofurans).

The HDO–HDN data show that *m*-cresol deoxygenation (HDO) is faster than *o*-ethylaniline denitrogenation (HDN), and this is in turn faster than indole denitrogenation

(HDN) under the same experimental conditions.

As far as we are aware, this is the first study in which the mutual interaction of catalytic HDO and HDN reactions is specifically addressed.

ACKNOWLEDGMENT

We acknowledge the support of the National Science Foundation.

REFERENCES

1. Katzer, J. R., and Sivasubramanian, R., *Catal. Rev. Sci. Eng.* **20**(2), 155 (1979).
2. Shah, Y. T., and Cronauer, D. C., *Catal. Rev. Sci. Eng.* **20**(2), 209 (1979).
3. Whitehurst, D. D., *et al.*, "Coal-liquefaction—The chemistry and technology of thermal processes." Academic Press, New York, 1980.
4. Rollmann, D. D., (a) Preprints *Amer. Chem. Soc. Div. Fuel Chem.* **21**(7), 59 (1976); (b) *J. Catal.* **46,** 243 (1977).
5. Whitehurst, D. D., *et al.*, "Exploratory studies in catalytic coal liquefaction." EPRI AF-Research Project 779-18, final report, May 1979.
6. Furimsky, E., *Amer. Inst. Chem. Eng.* **25**(2), 306 (1979).
7. Bertolacini, R. J., *et al.*, "Catalyst development for coal liquefaction report." Prepared for EPRI, Palo Alto, Calif. (1977).
8. McIlvried, H. G., *Ind. Eng. Chem. Process Des. Dev.* **10**(1), 125 (1971).
9. Sonnemans, J., *et al.*, *J. Catal.* **31,** 220 (1973); **34,** 215 (1974); **34,** 239 (1974).
10. Satterfield, C. N., and Cochetto, J. F., *AIChE J.* **21**(6), 1100, 1107 (1975).
11. Satterfield, C. N., *et al.*, *Ind. Eng. Chem. Process Des. Dev.* **17**(2), 141 (1978).
12. Gates, B., *et al.*, *AIChE J.* **55,** 129 (1978); **61,** 523 (1980).
13. Aboul-Gheit, A. K., and Abdou, I. K., *Inst. Petrol. J.* **59** (568), 188 (1973).
14. Goudriaan, H., *et al.*, *J. Inst. Petrol.* **59** (565), 40 (1973).
15. Cochetto, J. F., and Satterfield, C. N., *Ind. Eng. Chem. Process Des. Dev.* **20,** 49 (1981); **20,** 53 (1981).
16. Satterfield, C. N., and Gültekin, S., *Ind. Eng. Chem. Process Des. Dev.* **20,** 62 (1981).
17. Pauling, L., "Nature of the chemical bonds," 3rd ed., p. 85. Cornell University Press, Ithaca, N.Y., 1960.
18. Cotton, F. A., and Wilkerson, G., "Advanced inorganic chemistry," 2nd ed., p. 100. Interscience, New York, 1966.
19. Gates, G. C., and Broderick, D. H., *AIChE J.* **27**(4), 663 (1981).
20. Odebunmi, E. O., and Ollis, D. F., *J. Catal.* **80,** 56 (1983).
21. Odebunmi, E. O., and Ollis, D. F., *J. Catal.* **80,** 65 (1983).
22. Odebunmi, E. O., Ph.D. thesis, Princeton University, 1981.